

Hole-Confined Polar Optical Phonon Interaction in $\text{Al}_{0.35}\text{Ga}_{0.65}\text{As}/\text{GaAs}/\text{Al}_{0.25}\text{Ga}_{0.75}\text{As}$ Quantum Wells

Mohamed Boumaza^{1,*}, Yacine Boumaza²

¹Teacher Education college of Setif Messaoud Zeghar, Department of sciences, El Eulma, 19600, Algeria

²Batna 1 University, Department of Electrical Engineering, Faculty of Technology, 05000 DZ, Algeria

ARTICLE INFO

Article history:

Received: 19 March, 2022

Accepted: 15 May, 2022

Online: 25 May, 2022

Keywords:

Quantum Well

Confined Phonon

Semiconductor

ABSTRACT

In $\text{Al}_{0.35}\text{Ga}_{0.65}\text{As}/\text{GaAs}/\text{Al}_{0.25}\text{Ga}_{0.75}\text{As}$ quantum wells, the hole-confined polar optical phonon interaction is investigated. To calculate the valence band structure, we use the Luttinger-Kohn Hamiltonian with the k.p method. Within the dielectric continuum model, the hole-confined phonon scattering rates of intrasubband heavy holes in quantum well are calculated. It is found that the scattering rates are governed by an overlap integral and the density of states. Moreover, the scattering rates are reduced under compressive hydrostatic strain for low hole energy. The anisotropic effect on hole-confined phonon interaction is also studied.

1. Introduction

In physics, electron-phonon interaction plays an important role such as spin relaxation [1], superconductivity [2], quantum laser [3], mobility [4], Carrier thermalization [5]. Over the past decade, there has been an increasing interest of $\text{GaAs}/\text{Al}_x\text{Ga}_{1-x}\text{As}$ heterostructures with a variety of structures such as heterojunction [6], quantum well [7], quantum wire [8], quantum dot [9], multiquantum well [10], superlattice [11]. It is well known that phonons are confined in quantum well which has proven experimentally [12–14]. Furthermore, to describe the optical phonons in quantum well there are several models such as the dielectric continuum model (DCM) in [15], the hydrodynamic model in [16], the microscopic model in [17], and the hybrid model of in [18]. In the case of other structures such as periodic soliton we use the new generalized (G'/G)-expansion method [19].

In this paper, we calculate the valence band structure using the 6x6 Luttinger-Kohn Hamiltonian, taking into account the warping in $\text{Al}_{0.35}\text{Ga}_{0.65}\text{As}/\text{GaAs}/\text{Al}_{0.25}\text{Ga}_{0.75}\text{As}$ asymmetric quantum well [20,21] within the k.p method due to its simplicity and accuracy [22], whereas to describe the phonons in the quantum well, we use the dielectric continuum model which has been used by several authors [23–27], and given excellent results compared to the experimental results [28, 29]. In addition, we investigate hole confined phonon scattering rates for different quantum well

widths and the results are discussed. We also study the scattering rates under compressive hydrostatic strain using the theory of Luttinger–Kohn and Bir–Pikus [30].

2. Theory

In our work, we consider an asymmetric quantum well grown along the z direction. The 6x6 Luttinger Hamiltonian is transformed into two 3x3 matrixes [31,32], we calculate the hole band structure, by solving the Schrödinger equation including the heavy hole (HH), light hole (LH), and spin-orbit split-off subbands.

With the dielectric continuum model, the Frohlich Hamiltonian is written as [25]

$$H_{h-ph} = \sum_q \sum_m e\Phi_m(z) (a_m(q) + a_m^+(-q)) e^{iq \cdot r} \quad (1)$$

here $a_m^+(-q)$ is the phonon creation operator, $a_m(q)$ is the phonon annihilation operator, $\Phi_m(z)$ is the normalized phonon potential, r is the position vector in the xy plane, m denotes the LO mode order index and q is the in-plane phonon wave vector.

Using the Fermi's golden rule, the hole-confined phonon scattering rates from the initial hole state with the wave vector k_i within subband i to the final hole states in subband f with wave vector k_f are calculated as [33]

*Corresponding Author: Mohamed Boumaza, mboumazaphy1@gmail.com

$$\gamma_{i \rightarrow j} = \frac{2\pi}{\hbar} \int |M(f, i)|^2 \delta(E_f \pm \hbar\omega - E_i) dN_f \quad (2)$$

here, N_f is the number of final states, E_i is the initial hole state energie, E_f is the final hole state energie, $M(f, i)$ is the function connecting between the initial and the final hole states. Equation (2) yields

$$\gamma_{i \rightarrow j} = \frac{1}{2\pi\hbar} \frac{k_f}{\frac{\partial E_f}{\partial k}} (N_q + \frac{1}{2} \pm \frac{1}{2}) \Gamma_{if} \quad (3)$$

where N_q is the phonon occupation number, Γ_{if} is the function of the hole wave function and the phonon potential, which is written as

$$\Gamma_{if} = \sum_m \int \int |\langle f, k_f | e\Phi_m(z) | i, k_i \rangle dz|^2 d\theta \quad (4)$$

In Equation (4) the integration is done numerically where momentum and energy are conserved. The phonon potential $\Phi_m(z)$ is provided by [25]

$$\Phi_m(z) = A_c \cos\left(\frac{m\pi z}{L}\right) \quad m=1,3,5,.. \quad (5)$$

$$\Phi_m(z) = A_c \sin\left(\frac{m\pi z}{L}\right) \quad m=2,4,6,.. \quad (6)$$

here L is quantum well width, A_c is the normalization constant [25].

3. Results and discussions

In our work, we use the material parameters listed in Table [34–36]

Table 1: Parameters used in our work

Parameter	Unit	GaAs	AlAs
γ_1		6.85	3.69
γ_2		2.1	0.79
γ_3		2.9	1.4
Δ	eV	0.341	0.28
E_g	eV	1.424	2.671
a_v	eV	-1.16	-2.47
$\hbar\omega_{LO}$	eV	0.03625	0.05009

Figure 1 shows the valence band structure of a 25 Å $\text{Al}_{0.35}\text{Ga}_{0.65}\text{As}/\text{GaAs}/\text{Al}_{0.25}\text{Ga}_{0.75}\text{As}$ asymmetric quantum well in the $k_x - k_y$ plane showing a great nonparabolicity with lifted spin degeneracy. Because of the coupling between the heavy hole and light hole subbands, our results exhibit a strong anisotropy along the [10] and [11] directions. We note here that the heavy hole subband is more anisotropic than the light hole subband in particular for high energies.

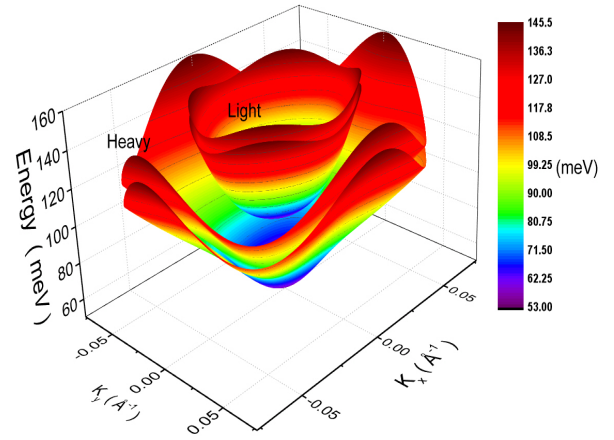


Figure 1: Heavy hole subband and light hole subband structures as a function of wave vector k in the $k_x - k_y$ plane for $L = 25$ Å and for clarity, the split off subband is not shown.

Figure 2.a shows the intrasubband heavy holes scattering rates $\gamma_{H \rightarrow H}$ of the confined optical phonon absorption as function of initial hole energy for different well widths, whereas the function Γ_{if} is shown in (b).

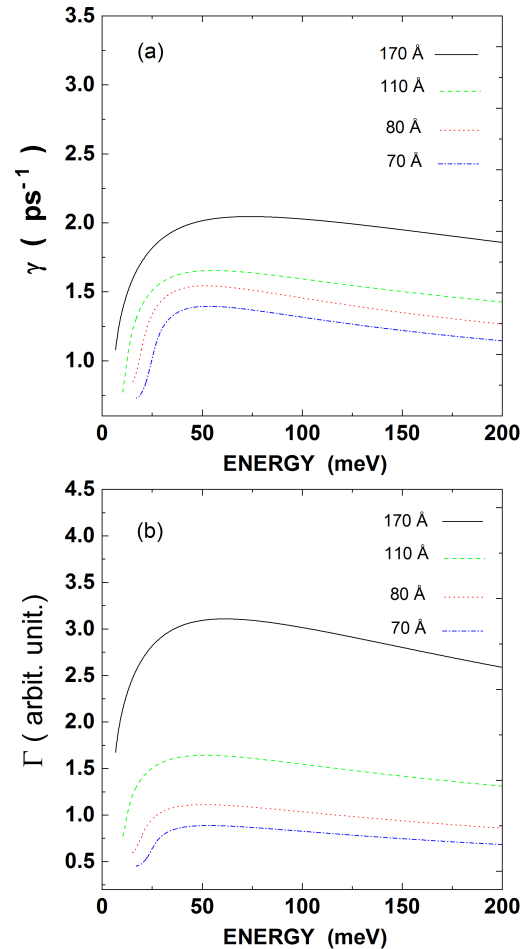


Figure 2: a) Intrasubband scattering rates of heavy hole for different well widths respectively 70 Å, 80 Å, 110 Å, 170 Å b) The function Γ_{if}

The scattering rates depend on the density of states and the function Γ_{if} . Therefore, to understand our results, we plot in Figure 3 the dependence of the density of states on the hole energies.

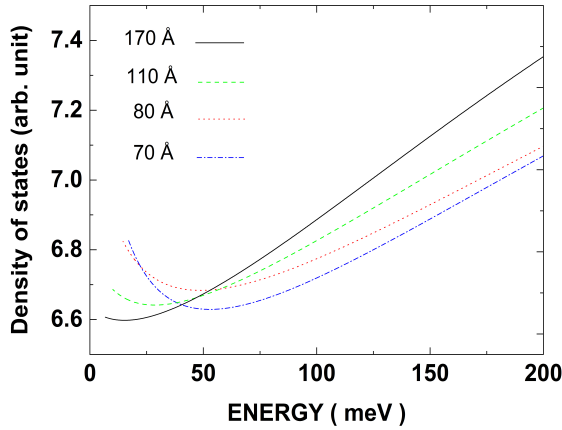


Figure 3: Density of states $D(E)$ of heavy hole as function of hole energy and for different well widths.

One can see that for low hole energy scattering rates increase rapidly with increasing hole energy to reach its maximum value. However, for high hole energies although the density of states increases with increasing hole energy, scattering rates show a very slight decrease. This indicates that the scattering rate shows only a weak dependence on the density of states. The maximum value of the scattering rate is $1.39 \times 10^{12} \text{ s}^{-1}$ for $L = 70 \text{ Å}$ while the scattering rate reaches its highest value $2.045 \times 10^{12} \text{ s}^{-1}$ for $L = 170 \text{ Å}$.

It is well known that under hydrostatic strain valence band structure is altered, which leads to a significant change in the scattering rate. In order to study the scattering rates under strain, we show in figure 4 a) Heavy hole scattering rates for the confined optical phonon absorption as function of the initial hole energy for two quantum well widths 70 Å and 170 Å b) The overlap integral Γ_{if} . The dashed lines depict the scattering rates for 2 % of compressive hydrostatic pressure, whereas the solid lines for the results in the absence of strain. For low hole energy and for quantum well width $L = 70 \text{ Å}$ ($L = 170 \text{ Å}$) scattering rates under strain are reduced by about 46.5 % (64 %), on the other hand, for high hole energy and for $L = 70 \text{ Å}$ ($L = 170 \text{ Å}$) scattering rates are increased by about 2.8 % (2.3 %). This behavior is similar to the function Γ_{if} .

Figure 5 shows the scattering rate for the confined optical phonon as a function of the initial two dimensional wave vector k with including the warping in the valence subband structure. For clarity, we also plot in Figure 6 and 7 the scattering rates for confined phonon absorption as a function of the initial hole wave vector k in polar coordinates for two well widths $L = 25 \text{ Å}$ and $L = 170 \text{ Å}$ respectively. One can see that for the quantum well width $L = 25 \text{ Å}$ our results exhibit significant anisotropic behavior for high hole energies between the directions $[0 1]$ and $[1 1]$, in which scattering rates increase by 14.7 %. However, for the quantum

well width $L = 170 \text{ Å}$ scattering rates decrease by 54.5 %. This anisotropy is due to the strong valence subband anisotropy.

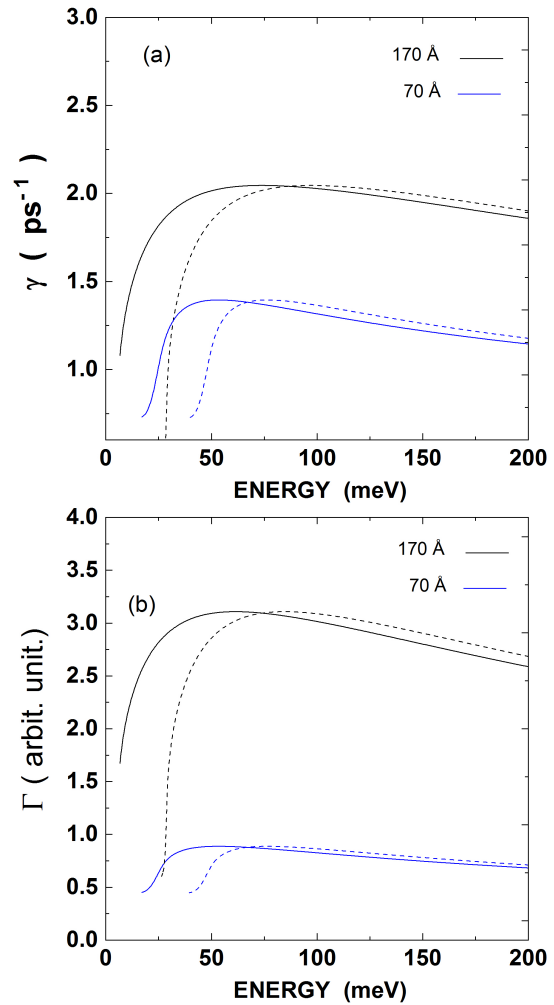


Figure 4: a) Scattering rates within heavy hole subband for the confined optical phonon absorption as function of the initial hole energy for two different well widths 70 Å and 170 Å b) The overlap integral Γ_{if} . The solid lines and dashed lines stand for the results without a strain with 2 % compressive hydrostatic pressure respectively.

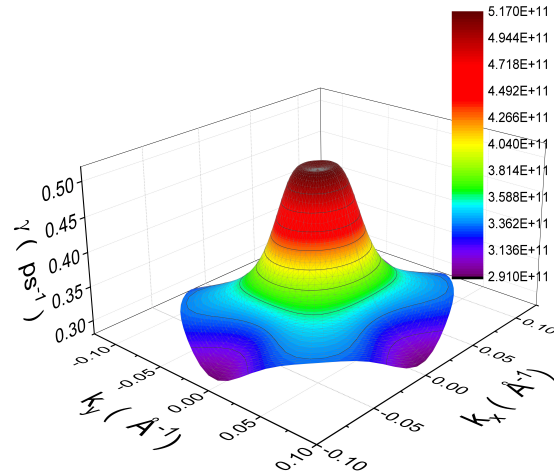


Figure 5: Scattering rates within heavy hole subband for confined optical phonon absorption with including warping as a function of the initial hole wave vector k in the k_x - k_y plane and for $L = 25 \text{ Å}$

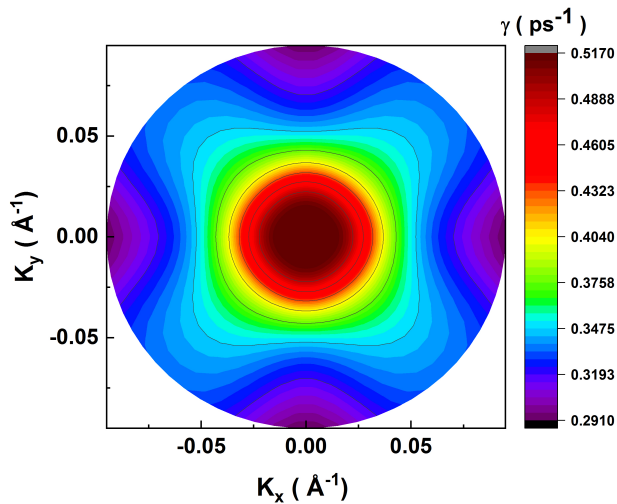


Figure 6: Scattering rates within heavy hole subband for confined optical phonon absorption as a function of the initial hole wave vector k in polar coordinates and for $L = 25 \text{ \AA}$

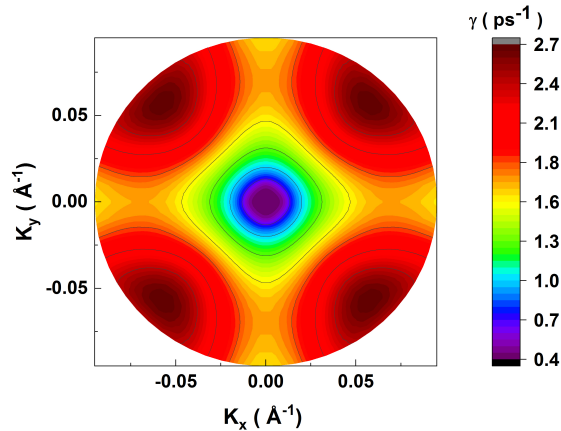


Figure 7: Scattering rates within heavy hole subband for confined optical phonon absorption as a function of the initial hole wave vector k in polar coordinates and for $L = 170 \text{ \AA}$

4. Conclusion

In summary, with the $k \cdot p$ method, the valence band structure is calculated including spin-orbit split-off subbands effect in the $\text{Al}_{0.35}\text{Ga}_{0.65}\text{As}/\text{GaAs}/\text{Al}_{0.25}\text{Ga}_{0.75}\text{As}$ asymmetric quantum wells. Hole-confined polar optical phonon scattering rates are investigated using the dielectric continuum model. It is found that scattering rates increase with increasing quantum well width. Moreover, under compressive hydrostatic strain, the scattering rates are reduced, in particular for low hole energy. In addition, scattering rates follow mostly the behavior of the overlap integral and exhibit a strong anisotropy for high hole energy. This anisotropy increases with increasing quantum well width. Our results show the importance of the band structure engineering quantum well via strain and within the asymmetric quantum well to reduce scattering rates and, consequently, the mobility of carriers can be increased. In the future, we will extend our work to different quantum well growth directions.

Conflict of Interest

The authors declare no conflict of interest.

References

- [1] J. Park, J.-J. Zhou, M. Bernardi, "Spin-phonon relaxation times in centrosymmetric materials from first principles," *Physical Review B*, **101**(4), 045202, 2020, doi:10.1103/PhysRevB.101.045202.
- [2] M. Li, Y. Fang, C. Kenney-Benson, L. Wang, "Superconductivity and electron-phonon interaction in $\text{Sr}_x\text{Bi}_2\text{Se}_3$ under pressure," *New Journal of Physics*, **23**(8), 083011, 2021, doi:10.1088/1367-2630/ac14cf.
- [3] A. Demić, Z. Ikonić, P. Dean, D. Indjin, "Dual resonance phonon-photon-phonon terahertz quantum-cascade laser: physics of the electron transport and temperature performance optimization," *Optics Express*, **28**(26), 38788–38812, 2020, doi:10.1364/OE.410014.
- [4] T. Nematirram, D. Padula, A. Landi, A. Troisi, "On the Largest Possible Mobility of Molecular Semiconductors and How to Achieve It," *Advanced Functional Materials*, **30**(30), 2001906, 2020, doi:10.1002/adfm.202001906.
- [5] A. Asgari, L. Faraone, "Thermal broadening of electron mobility distribution in $\text{AlGaIn}/\text{AlN}/\text{GaIn}$ heterostructures," *Journal of Applied Physics*, **114**(5), 053702, 2013, doi:10.1063/1.4813866.
- [6] A. Sužiedėlis, S. Ašmontas, J. Gradauskas, V. Nargelienė, A. Čerškus, A. Lučun, T. Anbinderis, I. Papsujeva, A. Narkūnas, B. Kundrotas, R. Rinkevičienė, "Peculiarities of Temperature Dependence of Detected Voltage by $\text{GaAs}/\text{Al}_{0.25}\text{Ga}_{0.75}\text{As}$ Heterojunction Microwave Diode Near Intervalley Crossover," *Materials Science*, **20**(2), 138–140, 2014, doi:10.5755/j01.ms.20.2.6319.
- [7] T. Kawazu, "Valence Band Mixing in $\text{GaAs}/\text{AlGaAs}$ Quantum Wells Adjacent to Self-Assembled InAlAs Antidots," *Journal of Nanomaterials*, **2019**, e5349291, 2019, doi:10.1155/2019/5349291.
- [8] K.D. Pham, C.V. Nguyen, N.N. Hieu, H.V. Phuc, B.D. Hoi, B.M.H. Hoa, L.T.T. Phuong, "Theoretical investigation of hot electron cooling process in GaAs/AlAs cylindrical quantum wire under the influence of an intense electromagnetic wave," *Optical and Quantum Electronics*, **50**(9), 342, 2018, doi:10.1007/s11082-018-1606-x.
- [9] S. Germanis, P. Atkinson, R. Hostein, S. Suffit, F. Margaillan, V. Voliotis, B. Eble, "Electrical control of optically pumped electron spin in a single GaAs/AlAs quantum dot fabricated by nanohole infilling," *Physical Review B*, **102**(3), 035406, 2020, doi:10.1103/PhysRevB.102.035406.
- [10] O. Kojima, T. Kita, M.J. Steer, R.A. Hogg, "Modulation of exciton states through resonant excitation by continuous wave lasers in a GaAs/AlAs multiple quantum well," *Journal of Physics D: Applied Physics*, **54**(33), 2021.
- [11] H. Eisele, L. Li, E.H. Linfield, "High-performance GaAs/AlAs superlattice electronic devices in oscillators at frequencies 100–320 GHz," *Applied Physics Letters*, **112**(17), 172103, 2018, doi:10.1063/1.5020265.
- [12] A.K. Sood, J. Menéndez, M. Cardona, K. Ploog, "Interface Vibrational Modes in GaAs/AlAs Superlattices," *Physical Review Letters*, **54**(19), 2115–2118, 1985, doi:10.1103/PhysRevLett.54.2115.
- [13] M.V. Klein, "Phonons in semiconductor superlattices," *IEEE Journal of Quantum Electronics*, **22**(9), 1760–1770, 1986, doi:10.1109/JQE.1986.1073174.
- [14] A.K. Sood, J. Menéndez, M. Cardona, K. Ploog, "Resonance Raman Scattering by Confined LO and TO Phonons in GaAs/AlAs Superlattices," *Physical Review Letters*, **54**(19), 2111–2114, 1985, doi:10.1103/PhysRevLett.54.2111.
- [15] R. Fuchs, K.L. Kliewer, "Optical Modes of Vibration in an Ionic Crystal Slab," *Physical Review*, **140**(6A), A2076–A2088, 1965, doi:10.1103/PhysRev.140.A2076.
- [16] M. Babiker, "Longitudinal polar optical modes in semiconductor quantum wells," *Journal of Physics C: Solid State Physics*, **19**(5), 683–697, 1986, doi:10.1088/0022-3719/19/5/008.
- [17] K. Huang, B. Zhu, "Dielectric continuum model and Frohlich interaction in superlattices," *Physical Review B*, **38**(18), 13377–13386, 1988, doi:10.1103/PhysRevB.38.13377.
- [18] B.K. Ridley, "Electron-hybridon interaction in a quantum well," *Physical Review B*, **47**(8), 4592–4602, 1993, doi:10.1103/PhysRevB.47.4592.
- [19] Md.K. Alam, Md.D. Hossain, M.A. Akbar, K.A. Gepreel, "Determination of the rich structural wave dynamic solutions to the Caudrey–Dodd–Gibbon equation and the Lax equation," *Letters in Mathematical Physics*, **111**(4), 103, 2021, doi:10.1007/s11005-021-01443-9.
- [20] P.C. Klipstein, Y. Livneh, O. Klin, S. Grossman, N. Snapi, A. Glozman, E. Weiss, "A $k \cdot p$ model of InAs/GaSb type II superlattice infrared detectors," *Infrared Physics & Technology*, **59**, 53–59, 2013, doi:10.1016/j.infrared.2012.12.009.
- [21] S. Rodriguez, J.A. López-Villanueva, I. Melchor, J.E. Carceller, "Hole confinement and energy subbands in a silicon inversion layer using the

- effective mass theory,” *Journal of Applied Physics*, **86**(1), 438–444, 1999, doi:10.1063/1.370749.
- [22] Z. Becer, A. Benneker, N. Sengouga, “Modeling Energy Bands in Type II Superlattices,” *Crystals*, **9**(12), 629, 2019, doi:10.3390/cryst9120629.
- [23] M. Boumaza, S. Lamari, “Anisotropic intrasubband hole scattering by polar optical phonon modes in thin GaAs/AlxGa1-xAs quantum wells,” *Superlattices and Microstructures*, **72**, 156–163, 2014, doi:10.1016/j.spmi.2014.03.049.
- [24] W.-D. Huang, G.-D. Chen, Y.-J. Ren, “Effect of ternary mixed crystals on interface optical phonons in wurtzite InxGa1-xN/GaN quantum wells,” *Journal of Applied Physics*, **112**(5), 053704, 2012, doi:10.1063/1.4748173.
- [25] N. Mori, T. Ando, “Electron–optical-phonon interaction in single and double heterostructures,” *Physical Review B*, **40**(9), 6175–6188, 1989, doi:10.1103/PhysRevB.40.6175.
- [26] J. Požela, K. Požela, V. Jucienė, “Scattering of electrons by confined interface polar optical phonons in a double-barrier heterostructure,” *Semiconductors*, **41**(9), 1074–1079, 2007, doi:10.1134/S1063782607090126.
- [27] A.M. Alcalde, G. Weber, “Scattering rates due to electron-phonon interaction in CdS1-xSex quantum dots,” *Semiconductor Science and Technology*, **15**(11), 1082–1086, 2000, doi:10.1088/0268-1242/15/11/312.
- [28] X. Zianni, C.D. Simserides, G.P. Triberis, “Electron scattering by optical phonons in AlxGa1-xAs/GaAs/AlxGa1-xAs quantum wells,” *Physical Review B*, **55**(24), 16324–16330, 1997, doi:10.1103/PhysRevB.55.16324.
- [29] V.V. Bondarenko, V.V. Zabudskii, F.F. Sizov, “Electron-phonon interaction and electron mobility in quantum-well type-II PbTe/PbS structures,” *Semiconductors*, **32**(6), 665–667, 1998, doi:10.1134/1.1187461.
- [30] Y. Kajikawa, “Optical anisotropy of (111)-oriented strained quantum-wells calculated with the effect of the spin-orbit split-off band,” *Journal of Applied Physics*, **86**(10), 5663–5677, 1999, doi:10.1063/1.371577.
- [31] D.A. Broido, L.J. Sham, “Effective masses of holes at GaAs-AlGaAs heterojunctions,” *Physical Review B*, **31**(2), 888–892, 1985, doi:10.1103/PhysRevB.31.888.
- [32] C.Y.-P. Chao, S.L. Chuang, “Spin-orbit-coupling effects on the valence-band structure of strained semiconductor quantum wells,” *Physical Review B*, **46**(7), 4110–4122, 1992, doi:10.1103/PhysRevB.46.4110.
- [33] B.K. Ridley, *Electrons and Phonons in Semiconductor Multilayers*, 2nd ed., Cambridge University Press, Cambridge, 2009, doi:10.1017/CBO9780511581496.
- [34] S. Boyer-Richard, F. Raouafi, A. Bondi, L. Pédesseau, C. Katan, J.-M. Jancu, J. Even, “30-band k-p method for quantum semiconductor heterostructures,” *Applied Physics Letters*, **98**(25), 251913, 2011, doi:10.1063/1.3600643.
- [35] I. Vurgaftman, J.R. Meyer, L.R. Ram-Mohan, “Band parameters for III–V compound semiconductors and their alloys,” *Journal of Applied Physics*, **89**(11), 5815–5875, 2001, doi:10.1063/1.1368156.
- [36] GaAs, AlAs, and AlxGa1-xAs: Material parameters for use in research and device applications: *Journal of Applied Physics*: **58**(3), Mar. 2022.